34th Annual International Conference of the IEEE EMBS
San Diego, California USA, 28 August - 1 September, 2012

An Interactive Implantable Vagal Nerve Stimulator for Real-Time Modulation of Cardiac Autonomic Control

David Wagner, Rich Shelton, David Adams, Jason Garlie, Kyoung-Suk Rhee, Peng-Sheng Chen and Shien-Fong Lin

Abstract— Previous studies have shown that the initiation of atrial tachyarrhythmias was associated with sympathovagal coactivation. The sympathovagal coactivation can also be a risk factor leading to enhanced susceptibility of atrial arrhythmias. Recently, it was demonstrated that continuous low-level cervical vagus nerve stimulation can reduce sympathetic nerve activity. Therefore, interactive stimulation of the vagus nerve that delivers stimulation only during increased sympathetic firing may have the potential to immediately decrease sympathetic nerve activity and prevent or stop atrial tachyarrhythmias. In this report, we demonstrate a design of an interactive vagus nerve stimulator (IVNS) which performs vagus nerve stimulation only at times of increased sympathetic nerve activity. The IVNS receives sympathetic nerve signal from the left stellate ganglion (LSG), and pre-processes it for threshold detection. A microcontroller integrates the number of threshold crossings over time to determine nerve activity, and deliver on-demand stimulation pulses to the vagus nerve. In order to monitor the proper operation of the IVNS, a commercial radiotransmitting device is included in the design to record LSG activity, record left thoracic vagus nerve activity, and validate the function of the microprocessor. Using the IVNS, we plan to test the hypothesis that interactive stimulation of the vagus nerve during high sympathetic nerve activity reduces sympathetic nerve activity and prevents the initiation of atrial tachyarrhythmias.

I. Introduction

Autonomic nerve activity modulation is an emerging therapy for cardiovascular disease including arrhythmias and heart failure [1-6]. An example of an arrhythmia that may be effectively treated with autonomic nerve activity modulation is atrial fibrillation. There is considerable evidence that the onset and persistence of atrial fibrillation is greatly influenced by autonomic nerve activities from the extracardiac and intracardiac nervous structures [7, 8] [6, 9-11]. In our laboratory, we have developed an approach for telemetric measurement of extracardiac and intracardiac nerve activities in ambulatory animals[7] [8-11] [12-14]. Results from our previous studies have shown that sympathovagal coactivation is associated with the initiation of atrial tachyarrhythmias, including atrial fibrillation. Furthermore, we have shown continuous low level vagal nerve stimulation to be an effective means of reducing sympathetic nerve activity and paroxysmal atrial tachyarrhythmias in canines[11].

These observations suggest that timely stimulation of the vagal nerve may have the potential to immediately decrease sympathetic nerve activity and prevent or stop atrial tachyarrhythmias. Here we report the design of an interactive vagal nerve stimulator which stimulates the vagal nerve at times of increased sympathetic nerve activity as recorded from the left stellate ganglion.

II. Methods

A. Principle of operation

A block diagram of the Interactive Vagal Nerve Stimulator (IVNS) is shown in Figure 1. A commercial telemetric transmitter (Data Sciences International, St. Paul, MN) is incorporated in the design to allow validation of the device operation. The nerve activity of the left stellate ganglion is sensed by a pair of coiled stainless steel wire electrodes connected to the IN+ and IN- inputs of the IVNS. A third electrode wire connected to the REF terminal is attached to the chest cavity to act as the reference. A buffered copy of the nerve activity is available at the OUT+ and OUT- terminals. The OUT+ and OUT- terminals are connected to the channel one input of the telemetry transmitter. The nerve activity is amplified, filtered, and full-wave rectified by the analog signal conditioning section of the IVNS. The resulting signal is fed to a voltage comparator circuit built into the microcontroller (PIC16LF1823). The microcontroller has a built in digital-to-analog converter (DAC) which feeds the other input of the voltage comparator. The firmware running in the microcontroller uses the DAC to set the threshold voltage that the input signal must exceed to be considered valid nerve activity. The threshold crossings

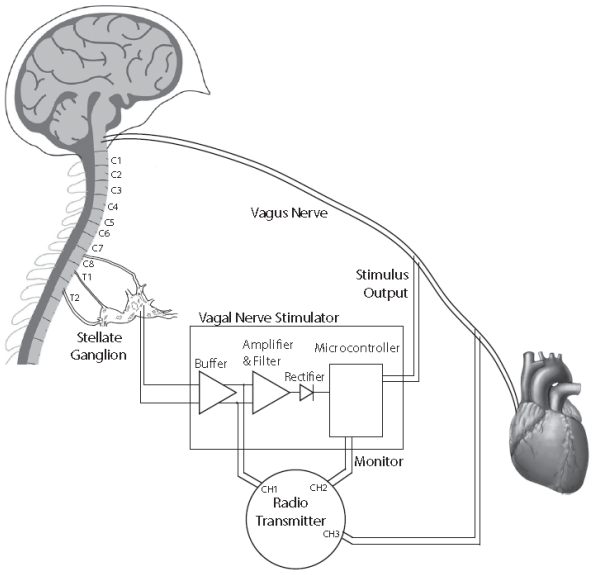

Figure 1: A schematic diagram of the IVNS device.

*Resrach supported by NIH R21 HL106554.

All authors are with the Krannert Institute of Cardiology, Indiana University School of Medicine. 1800 N. Capitol Ave., Indianapolis, IN 46202, USA. (phone: 317-962-0121, email: linsf@iupui.edu)

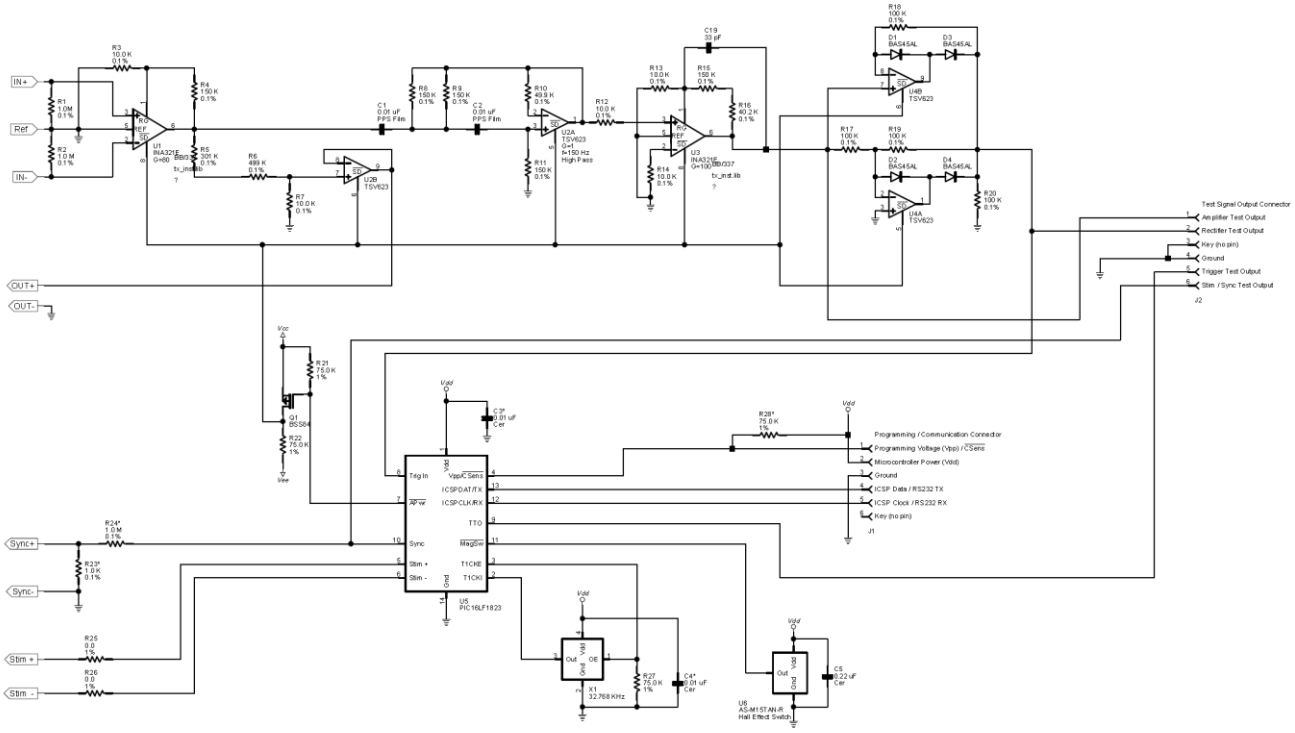

Figure 2: Schematic diagram of the IVNS device.

are counted and integrated over time to determine periods of high sympathetic nerve activity. When high activity is detected, the microcontroller will generate alternating bipolar stimulation pulses on the STIM+ and STIM- terminals. Electrodes from these terminals are attached to the left thoracic vagal nerve. For data recording purposes, a periodic timing pulse is generated by the microcontroller and output on the SYNC+ and SYNC- terminals. This timing pulse has two distinct patterns; one for times when stimulation pulses are being generated, and one for times when they are not. The channel two input of the telemetry transmitter is attached to the SYNC+ and SYNC- so this timing pulse can be recorded along with the nerve activity. The channel three input of the telemetry transmitter is attached to the vagal nerve downstream of the stimulating electrodes to record the effects of the stimulation.

B. Construction of the Interactive Vagal Nerve Stimulator

The analog signal conditioning section of the IVNS consists of a high gain differential instrumentation amplifier, a second order high pass filter, another high gain amplifier, and an absolute-value circuit. The total gain of the circuit is 8000. This value was experimentally determined to provide the highest possible signal level for the full wave rectifier while preventing saturation of the op-amp integrated circuit chosen for the rectifier. The frequency range of signals allowed to pass through the analog signal conditioning section of the IVNS is approximately 150 Hz to 10 kHz.

A schematic diagram of the circuit is shown in Figure 2. The differential amplifier, U1 in figure 2, is an INA321 type micro power CMOS Instrumentation Amplifier manufactured by Texas Instruments. The gain of the differential amplifier is set to 80 by resistors R3 and R4 along with resistors internal to the INA321 integrated circuit. Resistors R1 and R2 provide the required input bias current return path that keep the inputs within the amplifier's common-mode range. Resistors R5, R6, and R7 divide the output of the differential amplifier by approximately 80 and feed it to op-amp follower U2B. This provides a buffered copy of the stellate nerve activity to the telemetry transmitter for data recording. The high pass filter is made up of op-amp U2A, C1, C2, R8, R9, R10, and R11. This second order filter has a -3db cut off frequency of approximately 150 Hz. This is sufficiently high enough to eliminate most electrocardiogram and musculoskeletal signal components that may be picked up by the input leads.

The second amplification stage is built around another INA321 Instrumentation Amplifier. However, it is configured in a single ended mode. The gain of this stage is set at 100 by resistors R13, R15, and R16. Capacitor C19 causes this amplifier to act as a low pass filter by lowering the amplifier's gain for frequency components above 10 kHz. The final stage of the signal conditioning analog section is an absolute-value circuit, also known as a precision full-wave rectifier. The absolute-value circuit is needed because the voltage comparator built into the microcontroller only operates with positive going signals. The absolute-value circuit basically operates as a follower (U4B) and an inverter (U4A) whose outputs are ORed together through diodes D3 and D4. Positive inputs pass through U4B and D3. Negative inputs pass through U4A and D4. U4A is operated as a unity gain inverter so its output is the opposite polarity of its input. Diodes D1 and D2 limit the output swing of the amplifier not actively passing the signal so response time is improved.

The digital processing section of the IVNS is based on a PIC16LF1823 microcontroller (PIC chip) manufactured by

MicroChip Technology, Inc. (Chandler, AZ) It is a very low power consumption microcontroller with numerous built-in peripheral functions. Some of the peripherals used for this application are a 16-bit timer/counter, a voltage comparator, a digital-to-analog converter (DAC), and 12 general purpose input/output pins that can be individually configured as inputs or outputs. The auxiliary components surrounding the PIC chip (Q1, U6, and X1) perform these functions: Q1 allows the PIC chip to control the power-on or shutdown state of the signal conditioning analog section, U6 is a magnetic switch that allows the investigator to select the desired operating mode of the IVNS (explained below), and X1 is a 32.768 kHz crystal oscillator that is divided internally by the PIC chip to generate the time base used by the integration algorithm. An external oscillator was used so the PIC chip could be placed in a low power sleep mode when active processing wasn't needed. The integration time base continues to run while the PIC chip sleeps, then wakes up the PIC chip at the appropriate intervals.

The firmware running in the PIC chip performs two distinct functions. First, it controls the operating mode of the IVNS. Second, it performs the nerve activity integration algorithm to determine when and for how long to generate stimulation pulses. The IVNS operates in one of three modes; low power sleep mode, baseline recording mode, and full active mode. In the low power sleep mode, the signal conditioning analog section is in its powered down, the external crystal oscillator is turned off, the voltage comparator and DAC inside the PIC chip are disabled, the stimulate and sync outputs are off, and the PIC chip is placed in its sleep state. In this mode, minimum current is being drawn from the batteries. The first time a magnet is brought close to the magnetic switch, the PIC chip will wake and change the operating mode to the baseline recording mode. In the baseline recording mode, the signal conditioning analog section is turned on to allow the recording of stellate and vagal nerve activity without any stimulation pulses being generated by the IVNS. A periodic timing signal (20 ms on, 30 ms off) is output on the SYNC terminals to indicate the baseline recording mode is active. The second time a magnet is brought close to the magnetic switch, the operating mode will change to the full active mode, described below. A third magnetic switch event will set the operating mode back to the low power sleep mode.

When operating in the full active mode, the internal comparator of the PIC chip is set to monitor the filtered and rectified nerve activity. The internal DAC is sets the threshold voltage for the comparator. Every time the nerve activity signal exceeds the threshold voltage, the PIC chip increments a trigger count. The threshold voltage is set by the investigator at implant time. The PIC chip integrates these trigger counts over time to determine if stimulation pulses need to be generated. The 32.768 kHz clock signal from the external crystal oscillator is divided by a 16-bit timer/counter circuit within the PIC chip along with a software counter loop to produce a count window that is the basic integration period. This count window has a range of 50 milliseconds to 2.5 seconds, and is set by the investigator at implant time. During this count window, every time the nerve activity signal exceeds the threshold voltage, the trigger count is incremented. The PIC chip keeps a list of these trigger counts. At the end of a count window the counts are summed and compared to a count threshold value. If the summed counts exceed the count threshold value, a stimulation pulse will be generated. The number of trigger count values stored in the list and the count threshold value are both investigators configurable at implant time. As an example, let's assume the threshold voltage is 500 mV, the count window is 50 ms long, the number of trigger counts stored in the list is 5, and the count threshold is 12. At the end of the nth count window, trigger count C(n) will have a value of 4 if the nerve activity signal exceeded the threshold voltage four times. Let's assume the trigger counts for the previous four count windows are: C(n-1) = 5, C(n-2) = 3, C(n-3) = 1, and C(n-4) = 0. Summing these five trigger counts produces a value of 13, which exceeds the count threshold of 12, so a stimulation pulse will be generated. Even if the trigger count at the end of the n+1 count window is zero, a second stimulation pulse will be generated because C(n+1) + C(n) + C(n-1) + C(n-2) + C(n-3) would still be greater than the count threshold.

When commanded by the integration algorithm, the stimulation pulses will occur at a rate equal to the count window (50 ms in the example above). The investigator may specify the pulse duration at time of implant. The available duration times are 5, 10, 20, or 50 microseconds. The pulses generated on the STIM+ and STIM- pins are of alternating polarity. When no pulse is generated, both pins are in a high impedance state. During a stimulation pulse, one pin will be driven to the battery voltage of +3 volts and the other pin will be driven to the reference voltage (0 volts). During the next pulse, the polarities will switch. The one that was driven to battery voltage will be driven to reference, and vice-versa. This alternating on-state polarity coupled with the high impedance off-state produces pseudo bipolar stimulation pulses.

When the IVNS is operating in full active mode, a timing signal is generated on the SYNC+ pin that is fed to the channel 2 input of the telemetry device (SYNC- is reference). This timing signal is recorded along with the nerve activity to verify operation of the IVNS. The timing signal will be one

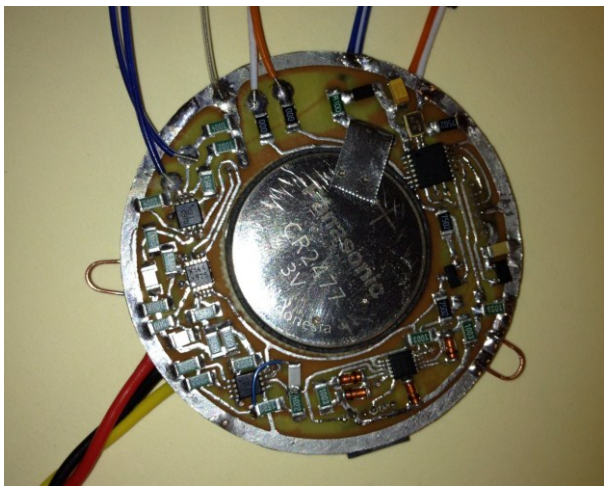

Figure 3: The device prior to being encapsulated in silicon for implantation.

of the two distinct patterns depending on if the IVNS is generating stimulation pulses. If the IVNS is not generating stimulation pulses, the timing pattern will be 10 ms ON followed by 40 ms OFF. If the IVNS is generating stimulation pulses, the timing pattern will be 10 ms ON, 10 ms OFF, 10 ms ON, and 20 ms OFF.

Two of the major considerations that went into the design of the IVNS were physical size and power consumption. The physical size and shape of the IVNS were determined by the fact it was to be implanted subcutaneously into a canine along with a commercially available telemetry transmitter. Since surgical procedures had already been established at our research facility to implant the telemetry transmitters, which are approximately 5 cm in diameter and 1 cm thick, a similar shape and size was chosen for the IVNS to simplify implant. Power consumption was the other major concern. The size and shape meant we had to use 3 Volt lithium button batteries to power the circuit. The experimental protocol dictated the IVNS would need to be placed in a low power consumption sleep mode for two weeks following implantation to allow the canine to heal. After that, it would be powered up and run in either a baseline recording mode or full active mode for up to 15 days. The electronic components were all chosen to minimize current consumption during both the sleep and powered on states.

We have constructed the device and performed preliminary studies in anesthetized dogs. An illustration of the completed circuit before encapsulated in silicon for the final implant is show in Figure 3. Various tests are conducted to ensure successful operation when the device is implanted in ambulatory animals. In preliminary tests, the IVNS correctly sensed enhanced nerve activity and generated pulses to stimulate the vagus nerve. Future data from ambulatory dogs will be used to test the hypothesis that interactive vagal nerve stimulation can promptly suppress the sympathetic activities.

III. Discussion

The approach of autonomic nerve stimulation as a treatment for atrial fibrillation has not yet been sufficiently evaluated. Some previous studies on vagal stimulation as a preventative treatment for atrial fibrillation have also been controversial in their results. In one study, stimulation of the vagosympathetic trunk shortened atrial refractory period and presumably made the atria more susceptible to arrhythmias [15]. In other studies, stimulation of the vagal nerve improved rate control of atrial fibrillation or increased the atrial fibrillation threshold from stimulation of the pulmonary vein region and presumably reduces the initiation of atrial fibrillation [5, 6]. Part of the limitations of these studies is that they were performed on animals under anesthesia, thus greatly reducing autonomic nervous system activity and the sensitivity of autonomic nervous system structures to stimulation. In our proposed studies, canines will be implanted with an interactive vagal nerve stimulator and a radiotransmitter to record nerve activity and then allowed to be ambulatory throughout the experiment. Our interactive vagal nerve stimulator will help in determining the role of autonomic nerve activity in the initiation and maintenance of atrial fibrillation. In addition, the development of this interactive nerve stimulator may be useful in studying other diseases that may be affected by autonomic nervous system activity. This may lead to many other diseases that may be effectively treated through autonomic nervous system modulation.

References

[1] G. M. De Ferrari, H. J. Crijns, M. Borggrefe *et al.*, "Chronic vagus nerve stimulation: a new and promising therapeutic approach for chronic heart failure," *Eur Heart J,* vol. 32, no. 7, pp. 847-55, Apr, 2011.

[2] P. J. Schwartz, "Vagal Stimulation for Heart Diseases: From Animals to Men: An Example of Translational Cardiology," *Circulation Journal,* vol. 75, no. 1, pp. 20-27, 2011.

[3] Z. F. Issa, X. Zhou, M. R. Ujhelyi *et al.*, "Thoracic spinal cord stimulation reduces the risk of ischemic ventricular arrhythmias in a postinfarction heart failure canine model," *Circulation,* vol. 111, no. 24, pp. 3217-20, Jun 21, 2005.

[4] J. C. Lopshire, X. Zhou, C. Dusa *et al.*, "Spinal cord stimulation improves ventricular function and reduces ventricular arrhythmias in a canine postinfarction heart failure model," *Circulation,* vol. 120, no. 4, pp. 286-94, Jul 28, 2009.

[5] S. Zhuang, Y. Zhang, K. A. Mowrey *et al.*, "Ventricular rate control by selective vagal stimulation is superior to rhythm regularization by atrioventricular nodal ablation and pacing during atrial fibrillation," *Circulation,* vol. 106, no. 14, pp. 1853-8, Oct 1, 2002.

[6] S. Li, B. J. Scherlag, L. Yu *et al.*, "Low-Level Vagosympathetic Stimulation: A Paradox and Potential New Modality for the Treatment of Focal Atrial Fibrillation," *Circ Arrhythm Electrophysiol,* vol. 2, no. 6, pp. 645-651, Dec 1, 2009.

[7] A. Y. Tan, S. Zhou, M. Ogawa *et al.*, "Neural mechanisms of paroxysmal atrial fibrillation and paroxysmal atrial tachycardia in ambulatory canines," *Circulation,* vol. 118, no. 9, pp. 916-25, Aug 26, 2008.

[8] M. J. Shen, E.-K. Choi, A. Y. Tan *et al.*, "Neural mechanisms of atrial arrhythmias," *Nat Rev Cardiol,* vol. 9, no. 1, pp. 30-39, 2012.

[9] M. J. Shen, E. K. Choi, A. Y. Tan *et al.*, "Patterns of baseline autonomic nerve activity and the development of pacing-induced sustained atrial fibrillation," *Heart Rhythm,* vol. 8, no. 4, pp. 583-9, Apr, 2011.

[10] E. K. Choi, M. J. Shen, S. Han *et al.*, "Intrinsic cardiac nerve activity and paroxysmal atrial tachyarrhythmia in ambulatory dogs," *Circulation,* vol. 121, no. 24, pp. 2615-23, Jun 22, 2010.

[11] M. J. Shen, T. Shinohara, H. W. Park *et al.*, "Continuous Low-Level Vagus Nerve Stimulation Reduces Stellate Ganglion Nerve Activity and Paroxysmal Atrial Tachyarrhythmias in Ambulatory Canines," *Circulation*, May 9, 2011.

[12] M. Swissa, S. Zhou, O. Paz *et al.*, "Canine model of paroxysmal atrial fibrillation and paroxysmal atrial tachycardia," *Am J Physiol Heart Circ Physiol,* vol. 289, no. 5, pp. H1851-7, Nov, 2005.

[13] B. C. Jung, A. S. Dave, A. Y. Tan *et al.*, "Circadian variations of stellate ganglion nerve activity in ambulatory dogs," *Heart Rhythm,* vol. 3, no. 1, pp. 78-85, Jan, 2006.

[14] M. Ogawa, S. Zhou, A. Y. Tan *et al.*, "Left stellate ganglion and vagal nerve activity and cardiac arrhythmias in ambulatory dogs with pacing-induced congestive heart failure," *J Am Coll Cardiol,* vol. 50, no. 4, pp. 335-43, Jul 24, 2007.

[15] D. P. Zipes, M. J. Mihalick, and G. T. Robbins, "Effects of selective vagal and stellate ganglion stimulation on atrial refractoriness," *Cardiovasc Res,* vol. 8, no. 5, pp. 647-655, September 1, 1974, 1974.